An observationally constrained model of strong magnetic reconnection in the solar chromosphere

***C. J. Díaz Baso**[1], J. de la Cruz Rodríguez[1], and J. Leenaarts[1]

[1] Institute for Solar Physics, Dept. of Astronomy, Stockholm University, AlbaNova University Centre, SE-10691 Stockholm, Sweden

*Email : carlos.diaz@astro.su.se

ABSTRACT

The evolution of the photospheric magnetic field plays a key role in the energy transport into the chromosphere and the corona. In active regions, newly emerging magnetic flux interacts with the preexistent magnetic field, which can lead to reconnection events that release magnetic energy, heating and accelerating the solar plasma. We use spectropolarimetric data at the Swedish 1-m Solar Telescope to study the heating caused by a strong reconnection event. The inversion of the data yielded a three-dimensional model of the reconnection event and surrounding atmosphere. The model atmosphere shows the emergence of magnetic loops with a size of several arcsecs into a pre-existing field. Where the reconnection region is expected to be, we see an increase in the chromospheric temperature of roughly 2000 K, bidirectional flows of the order of 10 km/s emanating from the region and plasmoids of roughly 0.2 arcsec diameter moving at velocities of order of 100 km/s. The chromospheric radiative losses at the reconnection site are as high as 160 kWm^{-2}, providing a quantitative constraint on theoretical models that aim to simulate reconnection caused by flux emergence.

1. Overview of observations

The NOAA 12593 was observed on 2016-09-21 from 11:00UT to 13:00UT (μ = 0.91) with the Swedish 1-m Solar Telescope (SST) in the Fe I 6301Å, Fe I 6302Å, Hα, Ca II 8542Å and Ca II K obtained with the CRISP and CHROMIS instruments. Inside the SST field-of-view (FOV) an emerging flux region was observed near the location of some pre-existent pores. At the location of the flux cancelation some brightenings are visible in chromospheric and coronal channels of the Solar Dynamics Observatory (SDO) Atmospheric Imaging Assembly (AIA) instrument (see **Fig. 1**), as well in the Ca II lines and Hα during the entire time-series of almost 2 hours. We have analized in detail the region of interest (ROI), indicated in **Fig. 2** as a green square.

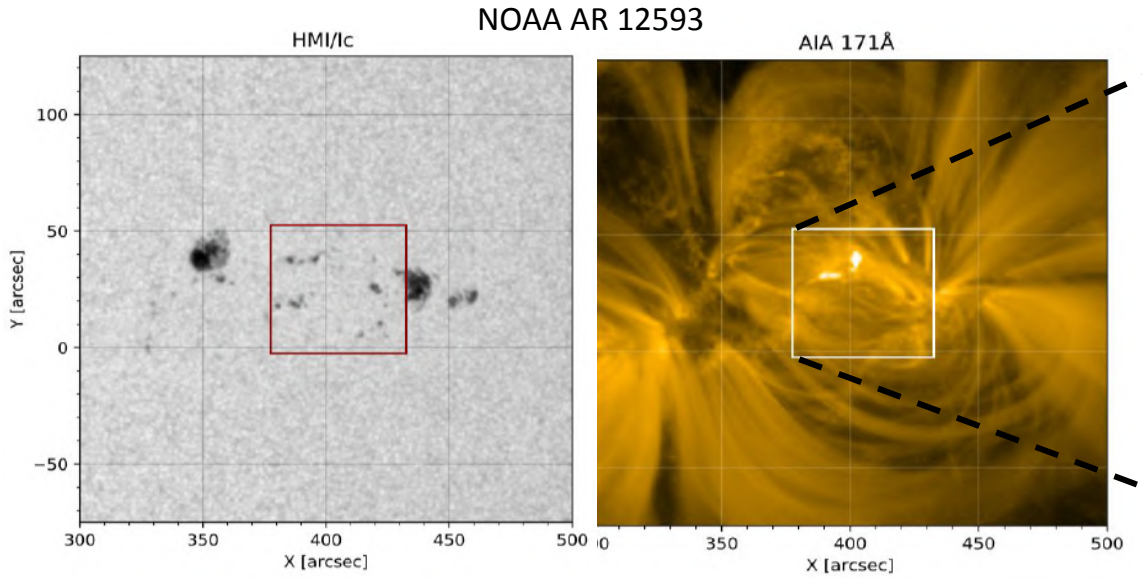

Fig. 1: Active region as seen from SDO-HMI and SDO-AIA channels. The square contour outlines the FOV covered by the SST.

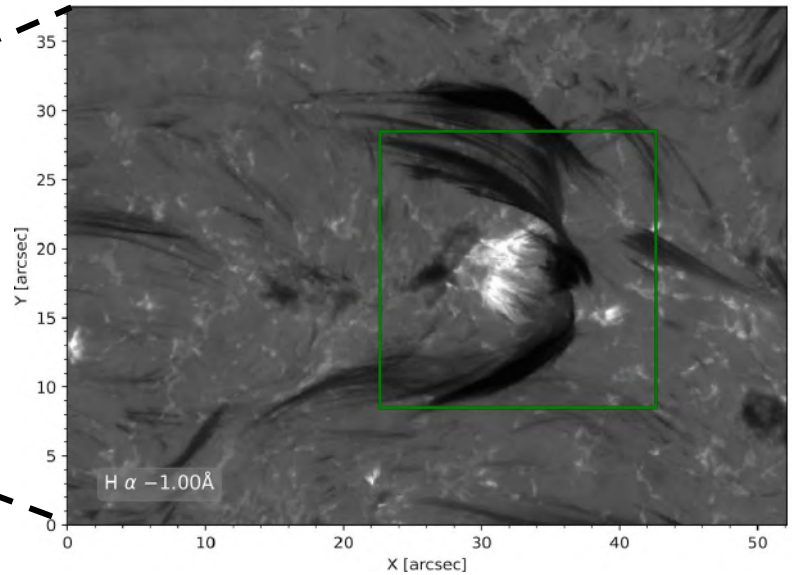

Fig. 2: FOV covered by the SST at two different wavelengths. The green square indicates the ROI and the black dashed square is a close-up for Fig. 5.

2. Atmospheric stratification: inversion of Stokes profiles

We performed an inversion of the Stokes profiles in the Fe I 6301.5 Å and 6302.5 Å, Ca II 8542 Å, and Ca II K lines simultaneously, using the parallel non-local thermodynamic equilibrium (NLTE) STockholm Inversion Code (STiC; de la Cruz Rodríguez et al. 2016, 2019).

The inversion yielded a three-dimensional model (x, y, logτ) of the reconnection event and surrounding atmosphere, including temperature, velocity, microturbulence, and magnetic file configuration, as shown in **Fig. 3**. The model atmosphere shows the emergence of magnetic loops with a size of several arcsecs into a pre-existing predominantly unipolar field.

We found an increase in the chromospheric temperature of roughly 2000K as well as bidirectional flows of the order of 10 km s^{-1} emanating from the region where the reconnection is expected. In the chromosphere there is an increase in the transverse magnetic field between the polarities that continues increasing to 1kG during the flux cancellation.

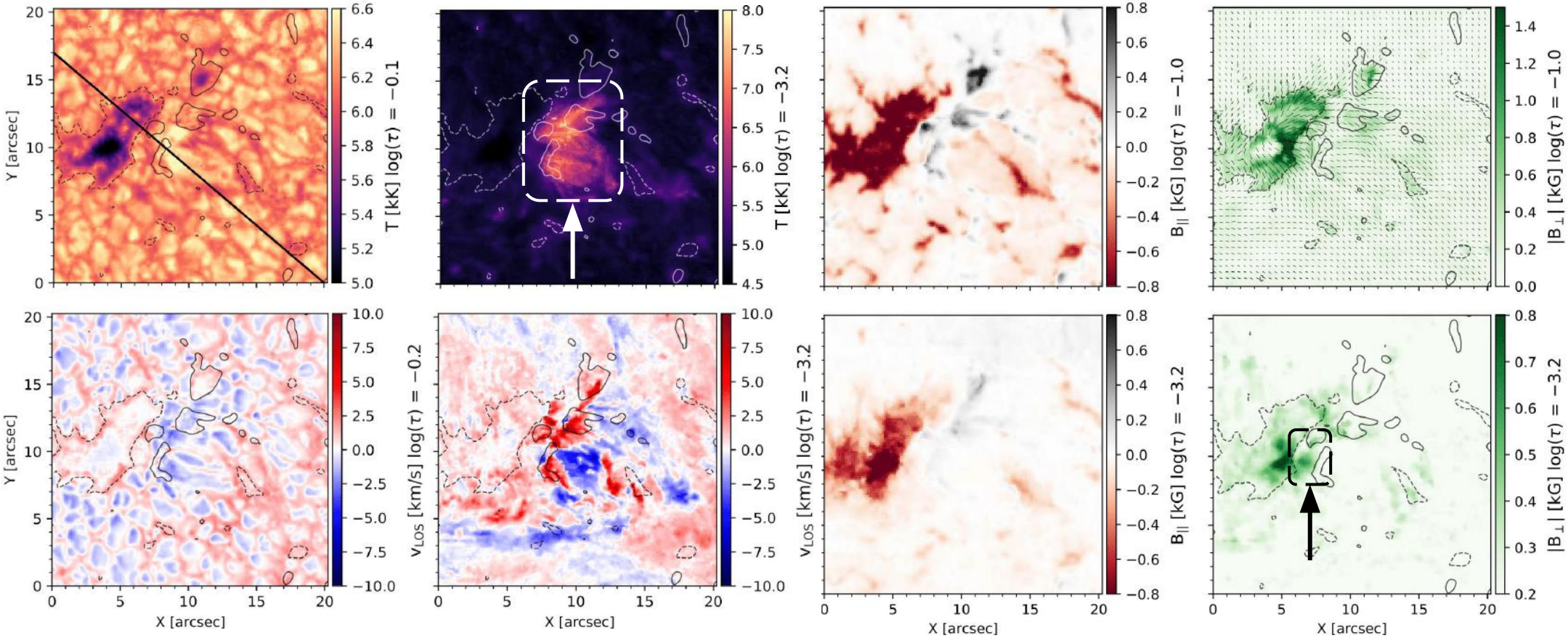

Fig. 3: Atmospheric structure in the ROI as inferred from the inversion. In columns at two different optical depths the temperature, the LOS velocity, the longitudinal magnetic field and the transverse magnetic field. The solid line indicates the cross-cut shown in Fig. 7.

3. Energy balance: estimates of heating rates

We estimated the total radiative cooling rate by summing the net cooling rates in bound–bound transitions for the spectral lines in our model atoms for Ca II and Mg II (approximation only valid for the low and mid-chromosphere).

Higher temperature regions correlate with enhanced radiative cooling. The total radiative losses ranges from ~4kWm^{-2} in the quiet sun (Vernazza et al. 1981), about ~30kWm^{-2} in intermediate areas, reaching peak values up to 160kWm^{-2} in the hottest region, as shown in **Fig. 4.**

The total integrated radiative losses during the two hours of observation is around ~5·10^{27} erg. The magnetic energy content using the magnetic field from the inversion is ~5·10^{29} erg, sufficient to sustain the chromospheric losses.

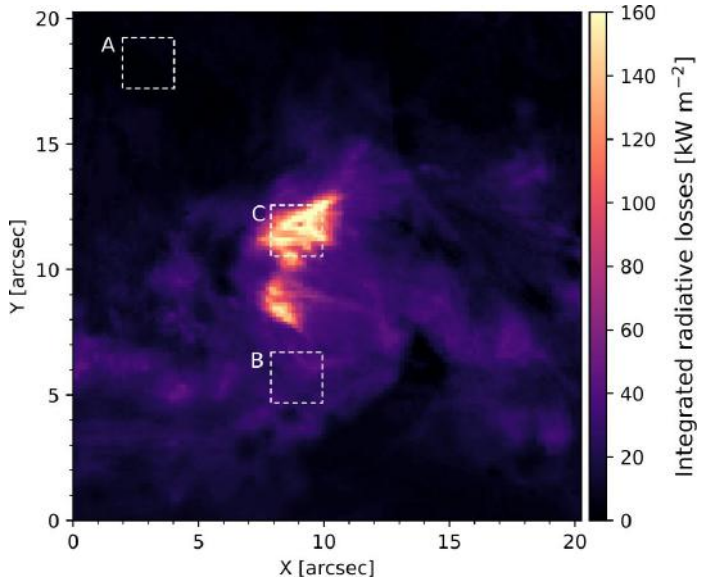

Fig. 4: Total integrated radiative losses.

4. Plasmoid-mediated magnetic reconnection

We detected many small-scale blobs with widths of around 0.2″, moving away from the cancelation site, identified in the blue wing (λ_0−1.3Å) of the Ca II K line, as shown in **Fig. 5.**

They have been identified as plasmoids (Rouppe van der Voort et al. 2017) as the result of the fragmentation of the current sheet involved in the reconnection event.

We detect fast transverse velocities of around 100 km/s similar to the LOS velocities indicating a tilted current sheet assuming that the flows are parallel to that.

We identified more than 25 similar blobs (in two consecutive frames): on average we have more than 1 blob every 30 seconds.

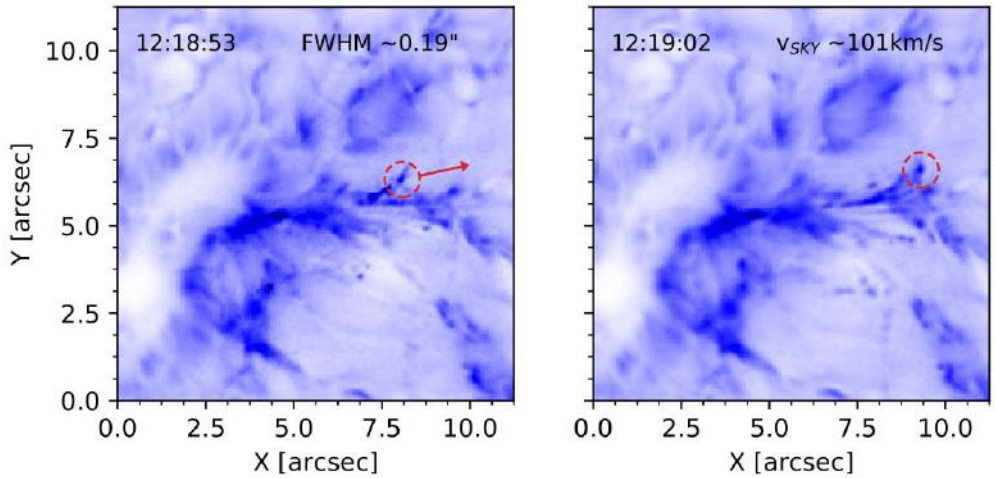

Fig. 5: Example of a blob in two consecutive frames.

5. Summary and magnetic field topology

The former analysis are suggestive of a model of magnetic reconnection between an emerging magnetic field and the pre-existing field similar to the classical emerging flux model for solar reconnection (Yokoyama & Shibata 1995) but on a much smaller scale where the event occurs deeper in the lower chromosphere (Hansteen et al. 2019).

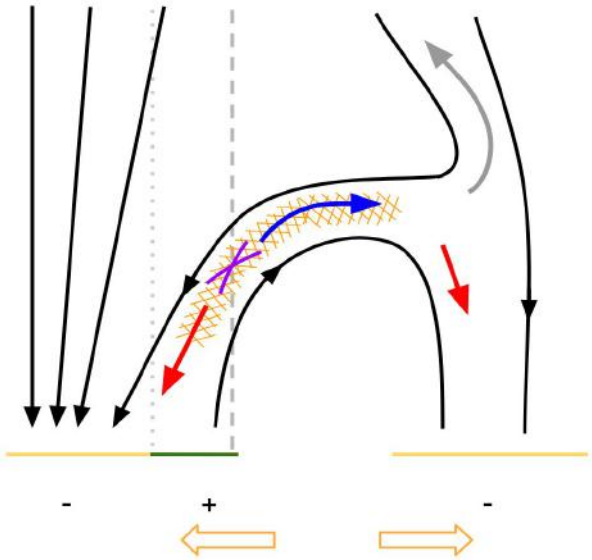

Fig. 6: Simplified illustration of the magnetic topology consistent with our results.

The sketch of **Fig. 6** schematically shows: (a) the emerged magnetic loop and the motion of the footpoints, (b) the pore with strong vertical fields, (c) the reconnection region with the corresponding heating and bidirectional flows, and (d) later plasma motions which escape from the region (gray arrow) or which fall again (right red arrow).

The dark jets observed in Hα at high velocity seem to match with the description of surges (Takasao et al. 2013; Nóbrega-Siverio et al. 2016).

To compare the similarities of our 2D sketch, we also show a cross-cut of the inversion results across the polarities in **Fig. 7.**

Increased brightness in the channels of SDO/AIA indicate heating associated with transition region and coronal temperatures. Our inversion is not sensitive above approximately 10000 K and we cannot set constraints on the height where the heating observed in AIA is located, but heating to transition-region temperatures in reconnection events higher in the chromosphere can give a response in AIA if the column density of overlying cool material is low enough (Guglielmino et al. 2019; Hansteen et al. 2019).

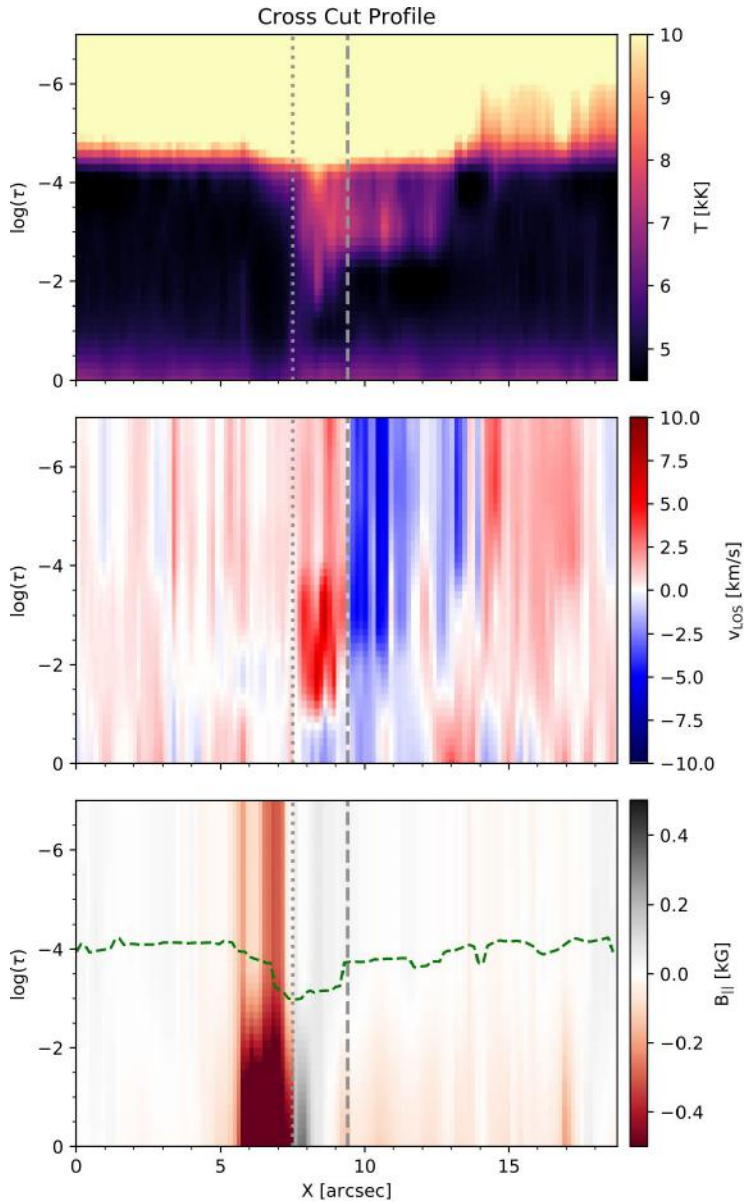

Fig. 7: Vertical stratification across the solid line indicated in the Fig. 3.

More info here: Díaz Baso et al, 2021, A&A 647, A188 (arxiv.org/2012.06229)

This project has received funding from the European Research Council (ERC) under the European Union's Horizon 2020 research and innovation programme (grant agreement 759548)